FLOW AND HEAT EXCHANGE IN THE SHAPING OF PROFILED FIBERS

V. M. Shapovalov

UDC 677.494:536.246:532.522

The article presents an analysis of tensile flow of profiled fibers under nonisothermal conditions. The effect of various factors on the shaping process is also analyzed.

The shape of the cross section of man-made fibers affects many of their properties: sorptional, their suitability for dying, abrasion resistance, thermal properties, gloss, etc. [1-3]. Most of the authors dealing with the question of changing the shape provide an analysis of the experimental results [1, 3, 4], and only Zyabitskii [2] suggested a model of change of shape of fibers with elliposidal section.

In investigating shaping, we did not take the profile of the drawing die as the initial configuration but the effective dimensions of the cross section of the jet, determined with distention taken into account. The analysis of three-dimensional flow in the drawing zone is substantially simplified by taking into account the condition $l \gg \sqrt{S/\pi}$ from which it follows, in particular, that the curvature of the surface of the jet in the longitudinal direction is much smaller than transversely. In consequence of this the radial component of the forces of aerodynamic friction is negligibly small. The environment does not take part hydrodynamically in providing a change of shape (shaping by the dry method). In the inertialess approximation the Navier–Stokes equations, describing the flow in the cross section of the jet, are linear. This enables us to view the velocity field as the superposition of flows due to uniaxial tension and to the action of capillary forces on the surface [5]. Thus the examined problem of changing shape in drawing profiled fibers is divided arbitrarily into two problems: the first is the isochoric change of shape of a cylindrical jet of viscous liquid under the effect of capillary forces; the second is uniaxial isochoric drawing of the jet in the zone of shaping.

Let the contour of a fiber with star-shaped section be approximated by the expression

$$R^* = q_0^* + \sum_{n=1}^{m} q_n^* \cos nZ\varphi, \tag{1}$$

where $Z = \pi/\varphi_0$. Under the effect of capillary forces, the contour of the fiber R^* tends to assume the shape of a circle with the radius $\sqrt{S/\pi}$, and then $q_n^* \to 0$, $q_0^* \to \sqrt{S/\pi}$. If we divide both sides of expression (1) by $\sqrt{S/\pi}$, we obtain

$$R = q_0 + \sum_{n=1}^{m} q_n \cos nZ\varphi, \tag{2}$$

where $q_0 = q_0^*\sqrt{\pi/S}$, $q_n = q_n^*\sqrt{\pi/S}$. From the equation of continuity we obtain the following equation of correlation between q_0 and q_n [6]:

$$q_0^2 = 1 - \frac{1}{4}\sum_{n=1}^{m} q_n^2 \tag{3}$$

We assume that viscosity over the cross section is uniform. The forces of inertia are much smaller than the forces of viscous friction. In addition, assume that σ, μ, S do not depend on time.

To determine q_n $(1 \leqslant n \leqslant m)$ as a function of time we use the equations of dynamics in Lagrange's form [6], and we regard the parameters q_n as generalized coordinates of the system

Volograd Polytechnic Institute. Translated from Inzhenerno-Fizicheskii Zhurnal, Vol. 47, No. 2, pp. 272-279, August, 1984. Original article submitted May 19, 1983.

 0022-0841/84/4702-0948$08.50

$$\frac{\partial U}{\partial q_n} = -\frac{\partial D}{\partial \dot{q}_n}, \quad n = 1, \ldots, m, \tag{4}$$

where $\dot{q}_n = dq_n/d\tau$, $\tau = (t\sigma/\mu)\sqrt{\pi/S}$.

On account of the symmetry, we will confine ourselves to examining the sector $0 \leqslant \varphi \leqslant \varphi_0$ with the length of the fiber equal to unity. The potential energy is determined by the integral

$$U = \int_0^{\varphi_0} \left[1 + \left(\frac{1}{R}\frac{\partial R}{\partial \varphi}\right)^2\right]^{1/2} R d\varphi.$$

Confining ourselves to the first two terms of the expansion of the integrand into a series, we obtain approximately

$$U = q_0 \frac{\pi}{Z} + \frac{\pi}{4} \sum_{n=1}^{m} Zn^2 q_n^2. \tag{5}$$

To determine the Rayleigh functions, we have to know the velocity field in the cross section. The Navier–Stokes equation has the form [7]

$$\nabla^2 (\nabla^2 \psi) = 0. \tag{6}$$

To attain correspondence with (2), we will seek the function ψ in the form

$$\psi_n = f_n(r) \sin Zn\varphi. \tag{7}$$

If we substitute (7) into (6), we obtain a differential equation for f_n:

$$r^4 f_n^{IV} + 2r^3 f_n''' - (1 + 2n^2Z^2) r^2 f_n'' + (1 + 2n^2Z^2) r f_n' + n^2Z^2 (n^2Z^2 - 4) f_n = 0. \tag{8}$$

From the solution of the Euler equation (8), taking the conditions $r = 0$, $v_r = 0$, $\partial v_r/\partial r = 0$ into account, we obtain for the function ψ [8]:

$$\psi_n = C_n r^{nZ+2} \sin Zn\varphi.$$

The constant C_n is determined from the condition that the radial velocity for $r = 1$ coincides with the velocity assumed in expression (2) [5, 6]. Thus the function of flow is determined by the expression

$$\psi = -\sum_{n=1}^{m} \frac{1}{Zn} \dot{q}_n r^{nZ+2} \sin Zn\varphi.$$

The Rayleigh function is determined by the integral

$$D = \frac{1}{2} \int_0^1 \int_0^{\varphi_0} \left[4\left(\frac{\partial v_r}{\partial r}\right)^2 + \left(\frac{\partial v_\varphi}{\partial r} + \frac{1}{r}\frac{\partial v_r}{\partial \varphi} - \frac{v_\varphi}{r}\right)^2\right] d\varphi r dr,$$

where $v_r = -(1/r)(\partial\psi/\partial\varphi)$, $v_\varphi = \partial\psi/\partial r$. If we integrate, we obtain

$$D = \frac{\pi}{Z} \sum_{n=1}^{m} \dot{q}_n^2 (Zn + 1). \tag{9}$$

Substituting expressions (5), (9) into (4), we obtain a system of differential equations of first order

$$\frac{dq_n}{d\tau} = -\frac{Z^2n^2}{4(nZ+1)} q_n, \quad n = 1, \ldots, m. \tag{10}$$

The solution of (10), with the condition $\tau = 0$, $q_n = q_{n,0}$ taken into account, has the form

$$q_n = q_{n,0} \exp\left[-\frac{n^2Z^2}{4(nZ+1)}\tau\right], \quad n = 1, \ldots, m. \tag{11}$$

Thus the solution of the problem of the change of shape of a cylindrical jet of viscous liquid under the effect of capillary forces has the form

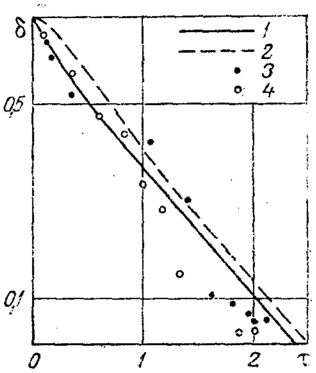

Fig. 1. Dependence of the dimensionless height of the ray on the dimensionless time of change of shape: 1) for configuration (a); 2) for configuration (b); 3, 4) experimental points [4] for G = 4.17•10^{-5} and 8.33•10^{-5} kg/sec, respectively.

$$R = q_0 + \sum_{n=1}^{m} q_{n,0} \exp\left[-\frac{n^2Z^2\tau}{4(nZ+1)}\right] \cos nZ\varphi, \tag{12}$$

where q_0 is a function of τ and is determined in accordance with (3) and (11). It can be seen from (12) that with an increase of the number of rays Z the rate of change of shape increases.

Figure 1 shows the dependence of the characteristic of the profile $\delta = (R^+ - R^-)/(R_0^+ - R_0^-)$ on τ for the cross sections presented in Fig. 2. When τ > 0.8 for profile *a* and when τ > 1.3 for b, there prevails the regular regime of change of shape, and there we may confine ourselves in calculations to the first term of the trigonometric polynomial (12). The rate of change of shape [9] depends on the number of rays

$$\frac{\partial \ln|R-1|}{\partial \tau} = -\frac{Z^2}{4(Z+1)}.$$

The results of numerical analysis of expression (12) for the star-shaped profile used by Gröbe and Versäumer [4], and for the fibers obtained by drawing dies in the shape of a circle with five rectangular grooves [3] are shown in Fig. 2a and b, respectively. As initial configuration of profile *a* the profile of the jet at the outlet from the die was taken. The contour was approximated by a section of a Fourier series (6 terms) by the 12-point method. In addition, the figure shows the profiles of the radial velocities of points of the surface for the instant τ = 0. The velocity of the surface was determined by differentiating expression (12) with respect to τ. The points lying in the acute angles of the section, where the largest curvature is found, have the highest velocity. The form of the theoretical profiles agrees qualitatively with the experimental results of [3, 4].

The investigation shows that the degree of transformation of the profile is characterized by the dimensionless time of change of shape. This characteristic is universal and may be used for evaluating the change of shape of fibers of any configuration. In particular the magnitude of τ characterizes the final configuration of the profile, and therefore the next problem is the calculation of τ under the conditions of freezing of the drawn fiber.

Let us examine part of the shaping path with length dx. The time within which a fiber passes this part is dt = dx/v. Flow on the part dx is isochoric. The increment of dimensionless time of change of shape is

$$d\tau = \frac{\sigma}{\mu v}\sqrt{\frac{\pi}{S}}\,dx. \tag{13}$$

The obtained differential equation enables us to determine τ if we know the dependences of σ, μ, v, S on the distance, therefore it has to be supplemented by the equations of motion and heat exchange of the fiber in the zone of drawing.

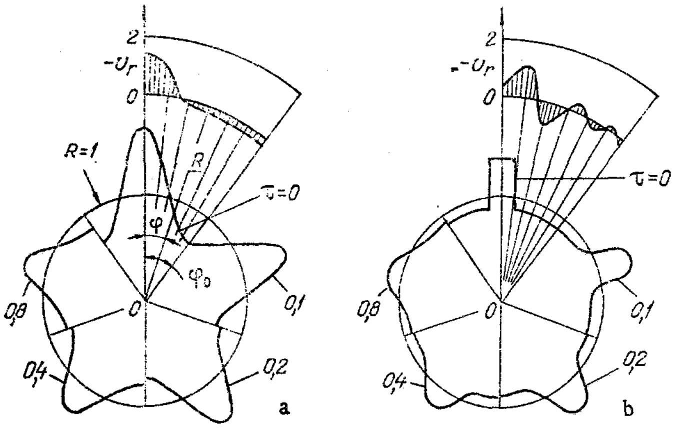

Fig. 2. Capillary transformation of fibers with different profiles in dimensionless representation: a) profile used in [4]; b) in [3].

In accordance with the theory of A. Zyabitskii, the balance of forces acting on the fiber [2]:

$$\frac{d}{dx}(SP_{xx}) - G\frac{dv}{dx} - \Pi P_{xx,s} + \rho g S = 0 \tag{14}$$

includes the forces: of rheological resistance $d/dx(SP_{xx})$, of inertia $G(dv/dx)$, of aerodynamic friction $\Pi P_{xx,s}$, and of gravity ρgS. We neglect the forces of surface tension in the longitudinal direction.

At present there do not exist any investigations of aerodynamic friction and heat exchange of profiled fibers; we therefore use the results obtained for circular fibers, and introduce the equivalent diameter of profiled fibers.

The stress in consequence of aerodynamic friction is determined as

$$P_{xx,s} = \frac{1}{2}\rho_c v^2 C_f$$

where $C_f = A\,Re^{\gamma}$. The characteristic linear dimension in Re is the equivalent diameter

$$d = \frac{4S}{\Pi} = \frac{2}{\Phi}\sqrt{\frac{G}{\pi\rho v}}, \tag{15}$$

where $S = \frac{G}{\rho v}$, $\Pi = 2\Phi\sqrt{\frac{\pi G}{\rho v}}$, $\Phi = 1 + \frac{Z^2}{8}\sum_{n=1}^{m} q_n^2$.

When fibers are shaped, the change of viscosity of the polymer with temperature is usually so great that the effect of nonlinearity of the flow considerably decreases. We assume that the tensile stress P_{xx} depends on the gradient of velocity and temperature

$$P_{xx} = 3\mu\frac{dv}{dx}, \text{ where } \mu = \mu_0 \exp\left[\frac{E}{R_1}\left(\frac{1}{T} - \frac{1}{T_0}\right)\right].$$

taking it in the first approximation that Truton's relation [2] is correct for longitudinal viscosity.

We assume that the convective mechanism of heat exchange predominates. Then for an element of the path dx long, the area of heat releasing surface with a view to the effect of ribbing amounts to Πdx [10]. The heat balance equation, without taking the effects of crystallization and dissipation into account, has the form

$$GC_p\frac{dT}{dx} = -\alpha(T - T_c)\Pi. \tag{16}$$

The thermal effect due to the work of the capillary forces is negligible. Thus, for the temperature of polyamide fiber to rise by 1°K, profiled fibers have to have dimensions measuring hundredths of a micron, which is commensurable with the dimensions of macromolecules.

The heat-transfer coefficient is determined from the equation [2]

$$\mathrm{Nu} = B\,\mathrm{Re}^{\beta}.$$

The characteristic dimension in Nu and Re is determined in accordance with (15).

Equations (14) and (16) contain the criterion of configuration Φ which characterizes the effect of ribbing due to the rays. Consequently, the process of shaping affects both the dynamics of motion of the fiber in the zone of drawing and the intensity of its cooling.

We introduce the dimensionless parameters: $X = x/l$, $V = v/v_0$, $\theta = (T - T_c)/(T_0 - T_c)$. Then Eqs. (13), (14), (16) assume the form

$$\tau' = \frac{\mathrm{Re}_1}{\mathrm{We}\sqrt{V}} \exp\left[\frac{E}{R_1}\left(\frac{1}{T_0} - \frac{1}{\theta(T_0 - T_c) + T_c}\right)\right],$$

$$\Gamma' = \frac{\Gamma^2}{V} - \frac{\mathrm{Re}_2^{\beta} E \Gamma V^{0.5\beta} \Phi^{2-\beta}\theta}{\mathrm{Gr}\, R_1 (T_0 - T_c)\left(\theta + \dfrac{T_c}{T_0 - T_c}\right)^2} + \tag{17}$$

$$+ \mathrm{Re}_1 (V\Gamma + \mathrm{Re}_2^{\gamma}\xi V^{2.5+0.5\gamma}\Phi^{1-\gamma} - \mathrm{Fr}) \exp\left[\frac{E}{R_1}\left(\frac{1}{T_0} - \frac{1}{\theta(T_0 - T_c) + T_c}\right)\right],$$

$$V' = \Gamma,\ \theta' = -\frac{\mathrm{Re}_2^{\beta}}{\mathrm{Gz}}\Phi^{2-\beta}\theta,$$

where

$$\mathrm{Re}_1 = \frac{\rho v_0 l}{3\mu_0};\ \mathrm{Re}_2 = \frac{2}{\nu_c}\sqrt{\frac{v_0 G}{\pi\rho}};\ \mathrm{We} = \frac{3v_0}{\sigma}\sqrt{\frac{\rho G v_0}{\pi}};\ \mathrm{Fr} = \frac{gl}{v_0^2};$$

$$\mathrm{Gz} = \frac{G C_p}{l\lambda_c \pi B};\ \xi = A\rho_c l\sqrt{\frac{\pi v_0}{\rho G}}.$$

A prime denotes the derivative with respect to X. Equations (17) were obtained on the assumption that ρ, σ, E, C_p do not depend on the temperature. The boundary conditions for the system (17) are:

$$X = 0,\ \tau = 0,\ V = 1,\ \theta = 1;\ X = 1,\ V = K,\ \text{where } K = v_1/v_0. \tag{18}$$

A numerical analysis of the system (17), (18) was carried out by Euler's method on a "Nairi-3" computer. Adequacy was verified by comparing the calculated data with the experimental results of [4]. Its authors investigated the cross sections of polyamide-6 fibers extruded from dies with star-shaped openings. The fiber passed over a certain path length in air (l = 0.04-2.62 m), and then it was rapidly cooled in a liquid bath. With increasing path length in the air the cross sections became ever more circular. The calculations were carried out for the conditions: $\mu_0 = 10^2$ Pa•sec; $\sigma = 3.6 \cdot 10^{-2}$ N/m; T_0 = 548°K; T_c = 303°K; B = 0.325; E = 41.7 kJ/mole; β = 0.3; A = 0.65; γ = −0.7; v_1 = 9.167 m/sec. The results of the calculations are presented in Fig. 1. A comparison of the experimental and theoretical results shows that there is satisfactory agreement.

Figure 3 shows the distribution of various parameters over the length of the drawing zone. The calculations were carried out for the case l = 2.62 m, $G = 4.167 \cdot 10^{-5}$ kg/sec. It can be seen from the drawing that the most intense change of shape occurs in the direct vicinity of the die where the dwelling time is relatively long (the axial velocity is low) and the viscosity of the molten material is smallest. The process of changing shape proceeds more rapidly than the process of freezing. The fiber passes the path from the zone of intense shaping to the freezing point at high velocity, and regardless of the strong decrease of transverse dimensions, the profile of the fiber changes only slightly because viscosity continuously increases, and the dwelling time is short.

Khan [3] expressed the assumption that the capillary effects of transforming the profile can be reduced by increasing the speed of delivery. An analysis of Eqs. (17), (18) confirms this assumption. For instance, if the speed of delivery is increased 12 times, it leads to a decrease of τ by 10%. There is a very strong dependence of τ on the initial velocity of the jet. Calculations showed that if v_0 is reduced by half, it leads to a decrease of τ by a factor of 5.5 (v_1 and G are constant). This is due to the fact that with

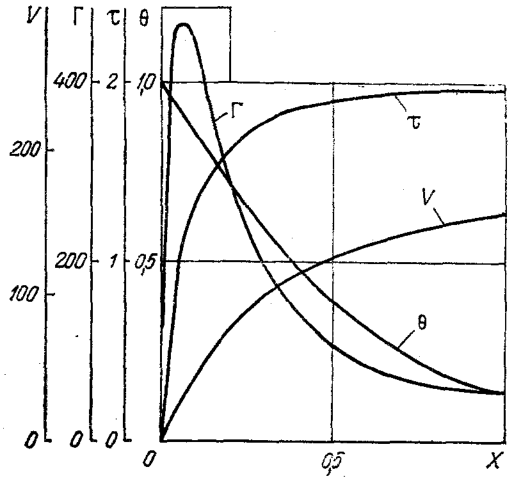

Fig. 3. Distribution of dimensionless parameters over the length of the shaping zone.

reduced initial velocity the dwelling time in the shaping zone decreases. Thus, the larger the cross section of the die is, the better is the shape of the profiled fibers retained. Retention of the shape of the fibers is also enhanced by increasing the activation energy and reducing the initial temperature of the melt.

The initial configuration of the fibers is greatly affected by the process of outflow from the die. Even if there is no distention (characteristic of high delivery speeds), the internal elastic stresses accumulated in the passage through the die may substantially change the configuration of the cross section of the fibers in the drawing zone. Determination of the initial profile of fibers entails considerable difficulties.

NOTATION

S, cross-sectional area; l, length of the drawing zone; R*, R, dimensional and dimensionless radius of the surface, respectively; q_n^*, q_n, dimensional and dimensionless generalized coordinates of the system, respectively; n, number of the harmonic; Z, number of rays in the cross section of the fiber; $2\varphi_0$, spread angle of one ray; U, dimensionless potential energy; D, dimensionless Rayleigh function; τ, dimensionless shaping time; $\dot{q}_n$, generalized velocity; ψ, function of flow; r, φ, cylindrical coordinates; f, function of the radius; C, constant; v_r, v_φ, velocity components; $q_{n,0}$, values of the parameters q_n at the instant $\tau = 0$; σ, surface tension; t, time; μ, shear viscosity; δ, dimensionless height of a ray; R^-, R^+, minimum and maximum running radius of the cross section, respectively; R_0^-, R_0^+, minimum and maximum radius of the cross section, respectively, at the instant $\tau = 0$; ∇^2, Laplace operator; x, X, longitudinal dimensional and dimensionless coordinate, respectively; v, V, dimensional and dimensionless axial velocity, respectively; μ_0, viscosity at the temperature T_0; E, activation energy; R_1, universal gas constant; T_0, T, initial and running absolute temperature, respectively; T_c, absolute ambient temperature; G, weight flow rate of the polymer; p_{xx}, tensile stress; $p_{xx,s}$, shear stress in consequence of aerodynamic friction; Π, length of the circumference of the fiber; g, acceleration of gravity; ρ, C_p, density and heat capacity, respectively, of the material of the fiber; θ, dimensionless temperature of the fiber; ρ_c, λ_c, ν_c, density, thermal conductivity, and kinematic viscosity, respectively, of the environment; v_0, initial axial velocity; α, heat-transfer coefficient; d, equivalent diameter; Re, Reynolds number; Re_1, Reynolds number for the fiber, Re_2, Reynolds number for the environment; We, Weber number; Fr, Froude number; Gz, Graetz number; Nu, Nusselt number; ξ, dimensionless parameter depending on the shaping conditions; K, real rate of drawing; A, B, β, γ, constants; Φ, criterion of configuration; Γ, gradient of axial velocity; v_1, speed of delivery; m, number of generalized coordinates.

LITERATURE CITED

1. G. Klare, E. Fritzsche, and V. Gröbe, Synthetic Polyamide Fibers [Russian translation], Mir, Moscow (1966).
2. A. Zyabitskii, Theoretical Foundations of Fiber Shaping [Russian translation], Khimiya, Moscow (1979).

3. Chang Dei Khan, Rheology in Conversion Processes of Polymers [in Russian], Khimiya, Moscow (1979).
4. V. Gröbe and H. Versäumer, "Über die Fadenbildung beim Schmelzspinnen. Teil 1," Faserforschung und Textiltechnik, 14, No. 6, 249-256 (1963).
5. L. I. Sedov, Mechanics of the Continuum [in Russian], Vol. 1, Nauka, Moscow (1973).
6. J. W. Strutt and Baron Rayleigh, The Theory of Sound, Peter Smith.
7. R. B. Bird, V. Stewart, and E. Lightfoot, Transport Phenomena, Wiley (1960).
8. L. É. Él'sgol'ts, Differential Equations and Variational Calculus [in Russian], Nauka, Moscow (1965).
9. A. V. Lykov, The Theory of Heat Conduction [in Russian], Vysshaya Shkola, Moscow (1967).
10. A. I. Veinik, Approximate Calculation of Heat Conduction Processes [in Russian], Gosudarstvennoe Énergeticheskoe Izd., Moscow–Leningrad (1959).

CURVED FLOW OF A VISCOUS LIQUID IN AN AXIRADIAL CHANNEL

Yu. E. Karyakin

UDC 532.542

The motion of a viscous liquid is an axiradial channel with curving of the flow is investigated with the aid of the implicit method of splitting according to spatial variables. The effect of the Reynolds number and of the intensity of the curving on the formation of regions of reverse flows is established.

The nature of the flow of a liquid or gas in turbine channels and various kinds of vortex installations depends largely on the initial curving of the flow and the regularity of its change. It was established [1] that even when a model of ideal gas in axiradial channels is used, regions with reverse flow may be obtained. The disposition and intensity of these regions are determined by the flow parameters at the inlet.

Tret'yakov and Yagodkin [2] investigated viscous curved flow of liquid in annular channels. They showed that the intensity of the curvature of the flow has a substantial effect on the magnitude of the frictional surface tension and the formation of zones of reverse flows.

The present work is an investigation of curved flow of a liquid in axiradial channels on the basis of the Navier–Stokes equations.

Let us examine the steady motion of a viscous incompressible liquid in an axiradial channel whose meridional section is formed by some piecewise smooth curved lines AB, BC, CD, and AD (Fig. 1). The z axis is the axis of symmetry of the channel.

We use a system of cylindrical polar coordinates. We assume that in the plane of the channel section there exists some pole O (R_0, z_0) for which the following correlation between the cylindrical (R, φ, z) and cylindrical polar coordinates (r, φ, θ) of an arbitrary point M (Fig. 1) exists: $R = R_0 - r\cos\theta$, $\varphi=\varphi$, $z = z_0 + r\sin\theta$, where φ is the azimuth angle.

The boundaries AD, AB, BC, and DC of the meriodional channel section are specified by the equations $\theta = \theta_1(r)$, $r = r_1(\theta)$, $\theta = \theta_2(r)$, $r = r_2(\theta)$, respectively. All these functions have to be piecewise smooth.

We assume that the flow is axisymmetric, and then we write the dimensionless Navier–Stokes equations of the examined laminar motion of an incompressible liquid in a system of cylindrical polar coordinates in the form

$$\frac{u}{r}\frac{\partial u}{\partial\theta} + v\frac{\partial u}{\partial r} + \frac{uv}{r} - \frac{w^2}{R}\sin\theta = -\frac{1}{r}\frac{\partial p}{\partial\theta} + \frac{1}{\mathrm{Re}}\left[\Delta u - \left(\frac{1}{r^2} + \frac{\sin^2\theta}{R^2}\right)u + \frac{2}{r^2}\frac{\partial v}{\partial\theta} + \left(\frac{1}{r} + \frac{\cos\theta}{R}\right)\frac{\sin\theta}{R}v\right], \quad (1)$$

M. I. Kalinin Leningrad Polytechnic Institute. Translated from Inzhenerno-Fizicheskii Zhurnal, Vol. 47, No. 2, pp. 280-285, August, 1984. Original article submitted May 30, 1983.

0022-0841/84/4702-0954$08.50